

Magnetic transitions induced by tunnelling electrons in individual adsorbed M-Phthalocyanine molecules ($M \equiv \text{Fe, Co}$)

Jean-Pierre Gauyacq^{1,2}, Frederico D. Novaes³, and Nicolás Lorente⁴

¹ CNRS, Institut des Sciences Moléculaires d'Orsay, ISMO,
Unité de Recherches CNRS-Université Paris-Sud, Bâtiment 351,
Université Paris-Sud, 91405 Orsay CEDEX, France

² Université Paris-Sud, Institut des Sciences Moléculaires d'Orsay,
ISMO, Unité de Recherches CNRS-Université Paris-Sud,
Bâtiment 351, Université Paris-Sud, 91405 Orsay CEDEX, France

³ Institut de Ciència de Materials de Barcelona (CSIC), Campus de la UAB, E-08193 Bellaterra, Spain

⁴ Centre d'Investigació en Nanociència i Nanotecnologia (CSIC-ICN),
Campus de la UAB, E-08193 Bellaterra, Spain

(Dated: November 10, 2021)

We report on a theoretical study of magnetic transitions induced by tunnelling electrons in individual adsorbed M-Phthalocyanine (M-Pc) molecules where M is a metal atom: Fe-Pc on a Cu(110)(2×1)-O surface and Co-Pc layers on Pb(111) islands. The magnetic transitions correspond to the change of orientation of the spin angular momentum of the metal ion with respect to the surroundings and possibly an applied magnetic field. The adsorbed Fe-Pc system is studied with a Density Functional Theory (DFT) transport approach showing that i) the magnetic structure of the Fe atom in the adsorbed Fe-Pc is quite different from that of the free Fe atom or of other adsorbed Fe systems and ii) that injection of electrons (holes) into the Fe atom in the adsorbed Fe-Pc molecule dominantly involves the Fe $3d_{z^2}$ orbital. These results fully specify the magnetic structure of the system and the process responsible for magnetic transitions. The dynamics of the magnetic transitions induced by tunnelling electrons is treated in a strong-coupling approach. The Fe-Pc treatment is extended to the Co-Pc case. The present calculations accurately reproduce the strength of the magnetic transitions as observed by magnetic IETS (Inelastic Electron Tunnelling Spectroscopy) experiments; in particular, the dominance of the inelastic current in the conduction of the adsorbed M-Pc molecule is accounted for.

PACS numbers: 68.37.Ef, 72.10.-d, 73.23.-b, 72.25.-b

I. INTRODUCTION

The development of Scanning Tunnelling Microscopy (STM) recently enabled to study the case of localised magnetic excitations at surfaces¹⁻⁷. Low-temperature STM experimental studies revealed that, in certain cases, a local spin could be associated with individual adsorbates at surfaces. Under the variation of the STM bias, the tip-adsorbate junction exhibits conductance steps at well-defined energies in the few meV energy range. These steps are attributed to the excitation of the local spin of the adsorbate and the step energy position yields the corresponding excitation energy, leading to magnetic IETS (Inelastic Electron Tunnelling Spectroscopy). Revealing the existence of nano-magnets at the atomic (molecular) level can have fascinating consequences for the miniaturisation of electronic devices. In addition, the possibility to determine the energy spectrum of the local spin on the adsorbate as a function of an applied magnetic B field provides an efficient way to quantitatively characterize the local spin and its interaction with the underlying substrate. This makes magnetic IETS an invaluable tool for magnetic studies of nano-objects at surfaces. In this respect, one can mention several spectacular results obtained in this way: evidence of spin coupling between neighbouring atomic adsorbates (anti-ferromagnetic coupling along adsorbed Mn

chains)², large magnetic anisotropy of atomic adsorbates (Mn and Fe adsorbates on CuN)³, change of magnetic structure of a molecular adsorbate on various substrates (Fe-Phthalocyanine on Cu and CuO)⁴, evidence of super-exchange interactions⁵, interaction of molecular adsorbates with magnetic substrates⁶, charging of adsorbed magnetic nano-objects⁷. Magnetic transitions could be easily evidenced in these systems due to the presence of a coating on the metal substrate that efficiently decouples the adsorbate from the continua of metallic states. When magnetic atoms are directly adsorbed on a metal, magnetic transitions could be observed but much broadened by the interaction with the substrate⁸.

Besides detailed insight into the structure of a magnetic adsorbate on a surface, IETS experiments bring also information on the dynamics of the excitation of a local spin by tunnelling electrons. Indeed, when considering a conductance spectrum as a function of the junction bias, the position of the conductance steps yields the excited state energies and the height of the conductance steps relative to each other and relative to the conductance at zero bias yields the relative magnitude of the various possible magnetic excitations. This feature is quite important for possible future applications, since it determines how easily a local adsorbate spin can be flipped at will by tunnelling electrons or can be quenched by collisions with substrate electrons⁹. It appears that magnetic tran-

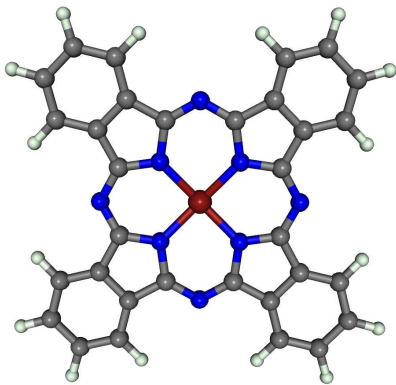


FIG. 1: Scheme of an M-Phthalocyanine molecule. In the present study M is taken as a Fe or a Co atom, here represented in red. The free molecule has a D_{4h} symmetry which is generally reduced upon adsorption on a substrate. The N-atoms are depicted in blue, C atoms in grey and H atoms in cyan.

sitions are highly probable²⁻⁵, much more probable than other inelastic processes like e.g. vibrational excitation by tunnelling electrons¹⁰⁻¹². As an extreme example, in the case of Co-Phthalocyanine (Co-Pc)⁵, the inelastic contribution to the current is found to be three times larger than the elastic current, whereas for vibrational excitation, the inelastic tunnelling contribution reaches at most a few per cent¹⁰⁻¹².

A few tools have been used to describe the spectroscopy and dynamics of a local spin on an adsorbate. First, the energy of a local spin interacting with its environment and possibly with an applied magnetic field, B , has been modelled efficiently with the following magnetic Hamiltonian¹³:

$$H = g\mu_B \vec{B} \cdot \vec{S} + DS_z^2 + E(S_x^2 - S_y^2), \quad (1)$$

where \vec{S} is the local spin of the adsorbate, g the Landé factor and μ_B the Bohr magneton. \vec{B} is an applied magnetic field. D and E are two energy constants describing the interaction of \vec{S} with the substrate, i.e. the magnetic anisotropy of the system. The Cartesian axis xyz are chosen according to the magnetic symmetries of the system. Hamiltonian (1) describes how the adsorbate spin, \vec{S} , is oriented in space due to its interaction with the substrate. The observed magnetic excitation energies of adsorbates were very efficiently modelled by the above Hamiltonian²⁻⁴. As for the strength of the magnetic excitations, it was first analyzed in a phenomenological way by Hirjebehidin *et al.*³. They showed that the relative heights of the inelastic conductance steps were very close to the relative magnitude of the squared matrix elements of the operator between the initial and final states of the transition. Nothing could be said about the relative magnitude of the elastic and inelastic conductance. This finding was later supported by several theoretical studies¹⁴⁻¹⁶

introducing in the description of electron tunnelling a coupling term proportional to the local spin. In first order perturbation theory, the inelastic current then appears proportional to the squared matrix elements of the coupling term between initial and final states, similarly to what was noticed in Ref. [3]. Recently, a completely different approach was introduced to treat magnetic excitations by tunnelling electrons¹⁷. It is based on the large difference of time scale between electron tunnelling and magnetic anisotropy of adsorbates: electron tunnelling is fast and the magnetic anisotropy can be considered as non-active during tunnelling. One can then describe tunnelling without the magnetic anisotropy taken into account and simply switch the latter at the beginning and at the end of tunnelling. In addition, DFT calculations on the two studied systems (Fe and Mn adsorbates on CuN) showed that only one coupling scheme between adsorbate and tunnelling electron spins is significantly contributing to tunnelling. The magnetic excitation appears as the result of a spin decoupling/recoupling process. This approach is non-perturbative and can then handle the large excitation probabilities encountered in these systems as well as make predictions for the elastic/inelastic relative contributions to tunnelling. In addition to bringing a qualitative view into the magnetic excitation process, it was shown to accurately account for the strength of the magnetic excitations, in particular relative to the elastic channel, in the case of Mn and Fe atomic adsorbates on CuN¹⁷. In the present work, we show how our method can be used in the case of Fe-Pc and Co-Pc molecules (Fig. 1) adsorbed on partly insulating substrates. As one of the main results, this approach is shown to precisely account for the overwhelming dominance of the inelastic conductance over the elastic conductance observed experimentally in these systems^{4,5}.

II. METHOD

We consider a local spin, \vec{S} , localized on an adsorbate on a surface. It is coupled to its environment by the Hamiltonian (1). Diagonalizing the Hamiltonian (1) yields the various spin states of the system, their energies, E_n , and the associated wave-functions, ϕ_n . Hamiltonian (1) is more easily written in the basis of $|S, M\rangle$ states, the eigenstates of \vec{S}^2 and S_z , so that the anisotropy states can be written as:

$$|\phi_n\rangle = \sum_M C_{n,M} |S, M\rangle \quad (2)$$

In the present study, we used the D , E and g parameters in Hamiltonian (1) as determined in the analysis of the experimental energy spectrum and from these, without any further parameter adjustment, we derive the strength of the magnetic transitions induced by tunnelling electrons. The various energy terms in Hamiltonian (1) are in the few meV range, so that one does not expect the

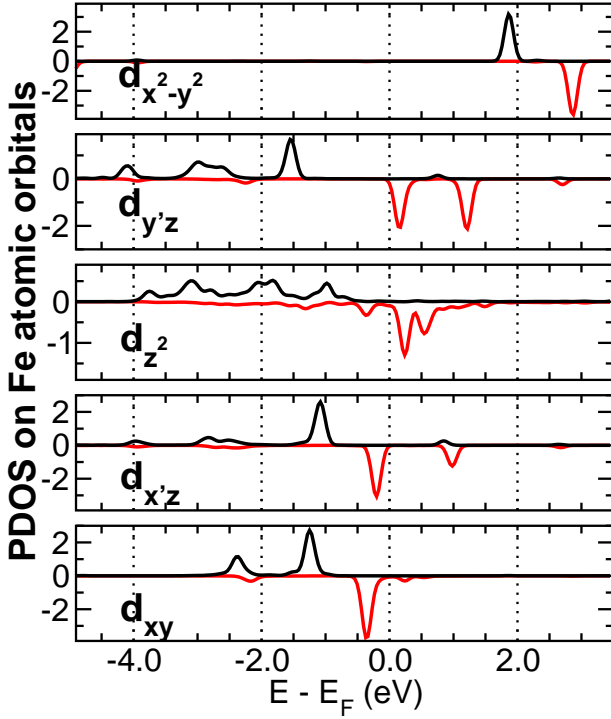


FIG. 2: Projected density of states (PDOS) on the Fe d -atomic orbitals. For all the curves shown here, the positive (black) curves corresponds to the majority spin, and the negative (red) to the minority spin. The d orbitals are classified according to the cartesian axes that contain the N–Cu–N axis of the molecule (x, y, z), or with respect to the surface directions: x' for the $[1 - 10]$ and y' for the $[001]$ directions. The z axis is the same for both reference frames.

corresponding interaction to play a role during the electron tunnelling process and one can treat this problem in the sudden approximation: treat the tunnelling without the magnetic anisotropy and then introduce it as a frame transformation at the beginning and at the end of tunnelling.

Electron tunnelling from the STM tip through the adsorbate and into the substrate (in the absence of magnetic anisotropy) can be represented by a scattering T matrix, noted $T_{Tip \rightarrow Sub}$ (and an equivalent one for the reverse tunnelling). It corresponds to the scattering of the tunnelling electron by the adsorbate and it depends on the electron energy. In the absence of magnetic anisotropy, it depends a priori on the spin coupling between the tunnelling electron and the adsorbate, via the exchange interaction. Thus, in the absence of significant spin-orbit interactions, it can be written in a diagonal form if we consider \vec{S}_T , the total spin of the system (electron + adsorbate). Defining $|S_T, M_T\rangle$ as the eigenfunctions of \vec{S}_T^2 and $S_{T,z}$ (if S is the adsorbate spin, then $S_T = S \pm \frac{1}{2}$), we can write formally the scattering $T_{Tip \rightarrow Sub}$ matrix (in the absence of magnetic anisotropy) as:

$$T_{Tip \rightarrow Sub} = \sum_{S_T, M_T} |S_T, M_T\rangle T_{Tip \rightarrow Sub}^{S_T} \langle S_T, M_T|. \quad (3)$$

$T_{Tip \rightarrow Sub}^{S_T}$ is a number, function of the electron energy. However, since, below, we consider only the limited energy range spanned by the magnetic excitations (up to 10 meV), the transmission probabilities $|T_{Tip \rightarrow Sub}^{S_T}|^2$ can be considered as constant in the present study. In the sudden approximation, the tunnelling amplitude (in the presence of magnetic anisotropy) is written as the matrix element of the $T_{Tip \rightarrow Sub}$ amplitude between the initial and final states of the tunnelling process. These states are written as $|\frac{1}{2}, m; \phi_n\rangle$ where the first part concerns the tunnelling electron (the electron spin is $1/2$ and m is the projection of the tunnelling electron spin on the quantization axis) and the second part concerns the local spin of the adsorbate. One then obtains the amplitude, $AMP_{m,n \rightarrow m',n'}$, for a tunnelling electron induced transition from ϕ_n to $\phi_{n'}$, while the tunnelling electron spin projection changes from m to m' as:

$$AMP_{m,n \rightarrow m',n'} = \sum_{S_T} T_{Tip \rightarrow Sub}^{S_T} \times \sum_{M_T} \langle \frac{1}{2}, m'; \phi_{n'} | S_T, M_T \rangle \langle S_T, M_T | \frac{1}{2}, m; \phi_n \rangle \quad (4)$$

One can see that there is a superposition (interference) of tunnelling amplitudes through the different S_T introduced by the magnetic anisotropy. Equation (4) yields the transition amplitudes in the general case, if the spin of the tunnelling electron is registered in both the initial and final states. Implicitly, it has been assumed above that the tunnelling electron quantization axis is the z -axis of the adsorbate magnetic anisotropy; situations with different quantization axis for the adsorbate and the tunnelling electron can be easily handled with an expression similar to Eq. (4).

We can now define the probability, P , for transitions from ϕ_n to $\phi_{n'}$ induced by unpolarized tunnelling electrons by summing incoherently over the distinguishable channels:

$$\begin{aligned} P_{n \rightarrow n'} &= \frac{1}{2} \sum_{m, m'} |AMP_{m,n \rightarrow m',n'}|^2 \\ &= \frac{1}{2} \sum_{m, m'} \left| \sum_{S_T} T_{Tip \rightarrow Sub}^{S_T} \right. \\ &\quad \times \left. \sum_{M_T} \langle \frac{1}{2}, m'; \phi_{n'} | S_T, M_T \rangle \langle S_T, M_T | \frac{1}{2}, m; \phi_n \rangle \right|^2. \end{aligned} \quad (5)$$

We can be a little more explicit by writing the total spin states, $|S_T, M_T\rangle$, as expansions over uncoupled spin states:

$$|S_T, M_T\rangle = \sum_m CG_{S_T, M_T, m} |S, M = M_T - m\rangle |\frac{1}{2}, m\rangle \quad (6)$$

where $|S, M\rangle$ states correspond to the adsorbate spin states and $|\frac{1}{2}, m\rangle$ to the tunnelling electron spin. Again, the adsorbate and electron spins are quantized on the same axis. The CG are Clebsch-Gordan coefficients. Combining (6) and (2) we can express the total spin states as an expansion over uncoupled products of adsorbate magnetic anisotropy states and tunnelling electron

spin:

$$|j\rangle = |S_T, M_T\rangle = \sum_{n,m} A_{j,n,m} |\phi_n\rangle |1/2, m\rangle \quad (7)$$

Equation (7) links the $|j\rangle = |S_T, M_T\rangle$, states appropriate to describe tunnelling without magnetic anisotropy to the channel states of the complete tunnelling process. We can then rewrite the transition probability (6) as:

$$P_{n \rightarrow n'} = \frac{1}{2} \sum_{m,m'} \left| \sum_{S_T} T_{Tip \rightarrow Sub}^{S_T} \sum_{M_T} A_{j,n,m} A_{j,n',m'}^* \right|^2. \quad (8)$$

In the case where the $T_{Tip \rightarrow Sub}^{S_T}$ tunnelling amplitude is dominated by a single symmetry, S_T (like it was found in the case of Mn and Fe adsorbates on CuN¹⁷, and like it is shown below to be the case in the systems studied here), the probability (8) further simplifies into:

$$P_{n \rightarrow n'} = \frac{1}{2} |T_{Tip \rightarrow Sub}^{S_T}|^2 \sum_{m,m'} \left| \sum_{M_T} A_{j,n,m} A_{j,n',m'}^* \right|^2. \quad (9)$$

This result, used in Ref. [17], is very simple, the electronic part of the tunnelling (the $T_{Tip \rightarrow Sub}^{S_T}$ amplitude) is factored out and the probabilities for the different channels are simply proportional to spin-coupling coefficients corresponding either to the magnetic anisotropy or to the coupling between electron and adsorbate spins (the coefficients are products of the diagonalization expansion coefficients in Eq. (2) and Clebsch-Gordan coefficients).

From the transition probabilities we can write the conductance dI/dV as a function of the STM bias, V , as:

$$\frac{dI}{dV} = C_0 \frac{\sum_n \Theta(V - EX_n) \sum_{m,m'} |\sum_j A_{j,1,n} A_{j,n,m'}^*|^2}{\sum_n \sum_{m,m'} |\sum_j A_{j,1,n} A_{j,n,m'}^*|^2}. \quad (10)$$

Expression (10) corresponds to the conductance for the system being initially in the ground state $n = 1$. The sum over n extends over all the $|\phi_n\rangle$ states, including the ground state, so that the above conductance takes all contributions, elastic and inelastic, into account. EX_n is the excitation energy of the magnetic level n , corresponding to the eigenvalue difference of the final, $|\phi_n\rangle$, and initial $|\phi_1\rangle$ states. The Heavyside function, Θ , takes care of the opening of the inelastic channels at zero temperature. C_0 is the total conductance corresponding to the transmission amplitude $T_{Tip \rightarrow Sub}^{S_T}$. It is then a magnetism-independent conductance. Since we only consider a limited V range, defined by the magnetic excitation energies, C_0 can be considered as constant in the relevant V -range. C_0 is equal to the conductance of the system for biases larger than all the inelastic thresholds. Expression (10) corresponds to the case where only one S_T value actually contributes to tunnelling so that the sum over j is restricted to the corresponding M_T values. If the two S_T symmetries contribute to tunnelling, a more general expression derived from Eq. (8) has to be used.

The above form (9) for the transition probabilities accounts for the strength of the magnetic transitions. In

fact, the transition probability is not proportional to a coupling term as in perturbation approaches, it appears as a simple sharing of the global transmission of the tip-substrate junction, $|T_{Tip \rightarrow Sub}^{S_T}|^2$, among the various spin states, $|\phi_n\rangle$. Qualitatively, in the magnetic excitation process, one can say that the incident electron arrives in a given spin state, it couples with the adsorbate spin to form a state of the total spin, S_T ; tunnelling through the junction occurs independently in the different total spins; at the end of the electron-adsorbate collision, the total spin splits back into its adsorbate and electron components, populating all the possible adsorbate spin states. Then, the expression for the sharing process (9) simply expresses angular-momentum conservation.

This kind of excitation process has been invoked in various situations where an exchange of angular momentum is involved: resonant rotational excitation in electron collisions on free and adsorbed molecules^{18,19}, spin-forbidden transitions in electron-molecule collisions²⁰ or in atom-surface scattering²¹. In all cases, it leads to efficient excitation processes. One can stress that this description of magnetic transitions is at variance with that of the vibrational excitation induced by collisional electrons^{22,23} or by tunnelling electrons²⁴⁻²⁶. However, even in the vibrational excitation case, a process similar to the one discussed here for magnetic transitions does exist. It is associated with the composition of the incident electron linear momentum with that of the target atom. Conservation of momentum leads to recoil of the target induced by electron scattering; however, due to the large ratio between electron and nuclei masses, the corresponding excitation is very weak and leads to very small excitation probabilities. Vibrational excitation has then to involve other processes such as e.g. resonant scattering, where the increase of the collision time allows weak interactions to be efficient in various situations of electron-molecule collisions^{22,23,27-31}. The above discussion can be summarized by stressing that the angular momenta (orbital or spin) of electrons and atoms or molecules can be of the same order of magnitude due to quantization (a few units in many cases) so that exchange between them is easy and has visible effects; in contrast, because of the large electron-nuclei mass ratio, the electron linear momentum is usually much smaller than that of heavy particles limiting the efficiency of momentum exchange processes. As a consequence, angular and spin degrees of freedom appear similar and the present treatment of spin transitions is very similar to the treatment of rotational excitation used in Ref. [19] to account for the experimentally observed efficiency of tunnelling electron in inducing molecular adsorbate rotations³².

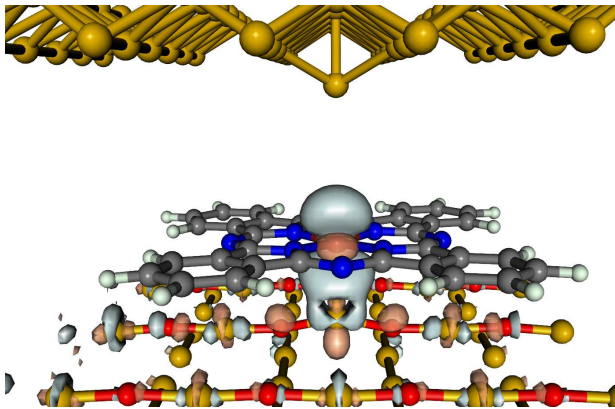


FIG. 3: Amplitude of the Kohn-Sham orbital of the Fe-Pc/Cu(110)(2 \times 1)-O + STM tip system at 0.2 eV above the Fermi level (positive in light grey and negative in light pink). The STM tip in the upper part is made of a Cu(110) surface with an extra protruding atom (in gold). The adsorbed Fe-Pc is lying flat on the substrate (N atoms in blue, C atoms in grey and H atoms in cyan). The substrate is in the lower part of the figure (Cu atoms in gold and O in red). The orbital is concentrated around the Fe atom and exhibits a strong d_{z^2} character perturbed by the interaction with the substrate.

III. MAGNETIC EXCITATIONS IN SUPPORTED Fe-PHTHALOCYANINE MOLECULES

Recently Tsukahara *et al*⁴ performed a detailed magnetic IETS study of single Fe-Phthalocyanine (Fe-Pc) molecules adsorbed on a Cu(110)(2 \times 1)-O surface. The molecule lay flat on the surface and two adsorption geometries were found, labelled α and β differing by the relative orientation of the molecule on the substrate. Clear magnetic transitions were observed by scanning the STM tip bias and were attributed to a local spin $S = 1$ interacting with the environment and with an applied magnetic field, B . The magnetic transitions were only observed when the tip was placed above the Fe atom and were attributed to a local spin of the Fe atom. The energies of the magnetic levels of the system as a function of the applied field were very precisely accounted for in Ref. [4] using Hamiltonian (1). The parameters of the two, α and β adsorption geometries are different: $D = -3.8$ meV, $E = 1.0$ meV and $g = 2.3$ for α -Fe-Pc and $D = -6.9$ meV, $E = 2.1$ meV and $g = 2.4$ for β -Fe-Pc, i.e. the same kind of structure but with a very different zero-field splitting of the magnetic states. We used this modelling of the magnetic structure to compute the strength of the magnetic excitations as induced by tunnelling electrons, making use of the formalism described in section II.

A. Electronic structure of the Fe-phthalocyanine molecule

A detailed description of the electronic structure of the Fe-Pc can be found in various references (see e.g. [33–35] and earlier references there in). The s outer electrons of the Fe atom are transferred to the surrounding Pc ring leaving a central Fe^{2+} ion with a $3d^6$ electronic configuration. In the free Fe-Pc, see Fig. 1, the Fe atom is surrounded by the Pc ring of D_{4h} symmetry, so that the Fe d manifold splits into b_{2g} (d_{xy}), e_g (d_{zx}, d_{yz}), a_{1g} (d_{z^2}) and b_{1g} ($d_{x^2-y^2}$) orbitals (the z -axis is normal to the Pc plane and the x and y -axis are parallel to the Fe-N interatomic axis). In the free Fe-Pc, the b_{2g} (d_{xy}) orbital is fully occupied, the b_{1g} ($d_{x^2-y^2}$) corresponds to the highest eigenenergy because of the large overlap with the N-atom orbitals, and four electrons occupy the e_g (d_{zx}, d_{yz}) and a_{1g} (d_{z^2}) orbitals. Various configurations have been proposed, with small energy differences between them (see a discussion in Ref. [35]). The structure of the other M-Pc (M = metal) is similar³⁵, a change of M along the Fe, Co, Ni, Cu and Zn sequence corresponding to the further filling of the split d manifold.

When the Fe-Pc is adsorbed on a Cu(110)(2 \times 1)-O surface, the D_{4h} symmetry is broken. If we assume the presence of the surface to only induce a perturbation on the structure of the free Fe-Pc, then the g subscript of the orbitals disappears and the e_g orbital splits (the d_{zx} and d_{yz} are not degenerate anymore). We will use the orbital notation of the free Fe-Pc when discussing the electronic structure of adsorbed Fe-Pc, although the molecules are distorted by the interaction with the surface.

B. Density functional study of Fe-Pc adsorbed on a Cu(110)(2 \times 1)-O surface

The ground state electronic structure configuration and the global transmission, $T_{\text{Tip} \rightarrow \text{Sub}}^{ST}$ for the tunnelling from an STM tip to the substrate passing through the Fe-Pc molecule were obtained by density functional theory (DFT) simulations, performed with the SIESTA and TRANSIESTA codes^{36,37}. We have used the generalized gradient approximation³⁸ for the exchange-correlation functional. We only studied the β adsorption geometry of the Fe-Pc on Cu(110)(2 \times 1)-O, which has a higher symmetry than the α geometry. The electronic structure in the α and β geometries are assumed to be equivalent.

Starting with the electronic structure analysis for the adsorbed molecule, SIESTA uses atomic orbitals for the basis set, and the projection of the density of states onto the Fe atomic orbitals reveals an open shell structure with two unpaired electrons, i.e. a $S = 1$ configuration ($d_{xy}^2 d_{y'z}^2 d_{z^2}^1 d_{x'z}^1$), as shown in Fig. 2. Note that the β adsorption geometry corresponds to the Fe-N axis rotated by 45° from the symmetry axis of the Cu(110) surface. As a consequence, the splitting of the e_g orbital by the substrate field involves x' and y' -axis rotated by 45°

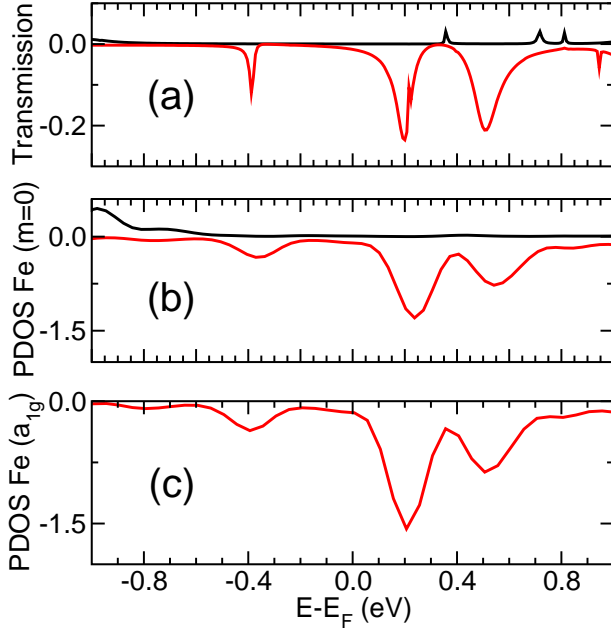


FIG. 4: In panel (a), the transmission function for the system shown in Fig. 3 as a function of the tunnelling electron energy (referred to the Fermi energy E_F) for a vanishing STM bias. Panel (b) shows the PDOS on the Fe d_{z^2} atomic orbital. Panel (c) shows the projection onto the a_{1g} molecular orbital of the free distorted Fe-Pc that corresponds to the d_{z^2} Fe orbital. Positive (black) curves correspond to the majority spin, and the negative (red) ones to the minority spin.

from the x and y -axis that correspond to the splitting of the d manifold by the interaction with the Pc ring. The projections in Fig. 2 were then performed on the appropriate symmetry orbitals i.e. the d_{xy} , d_{z^2} , $d_{x^2-y^2}$, $d_{zx'}$ and $d_{yz'}$ orbitals. More quantitatively, the computed spin polarization is 1.85 unpaired electrons. The corresponding spin is roughly $S = 1$, in good agreement with the experiment⁴. Due to its large overlap with the surface electronic structure, the d_{z^2} orbital is the one that hybridizes the most with the substrate.

Figure 3 shows the real space plot of the Kohn-Sham orbital at 0.2 eV above the Fermi level for the molecule+surface+STM tip system. This orbital corresponds to the peak in the PDOS onto the d_{z^2} Fe orbital (see Fig. 2). The strong d_{z^2} character of the orbital seen in Fig. 3 confirms that this orbital corresponds to the a_{1g} orbital perturbed by the substrate. The intuitive notion that, by reaching further out along the z -axis, this orbital would contribute more to the junction transmission is supported by comparing the transmission function (panel (a) of Fig. 4) with the PDOS onto the d_{z^2} Fe atomic orbital (b), and PDOS onto the molecular orbital a_{1g} of the Fe-Pc (c). Note that, for this projection, we used the a_{1g} orbital of the free Fe-Pc molecule, with the distorted atomic configuration of the adsorbed molecule. From this, it is clear that, at the Fermi level, the transmission is essentially made of the tail of the a_{1g} resonance

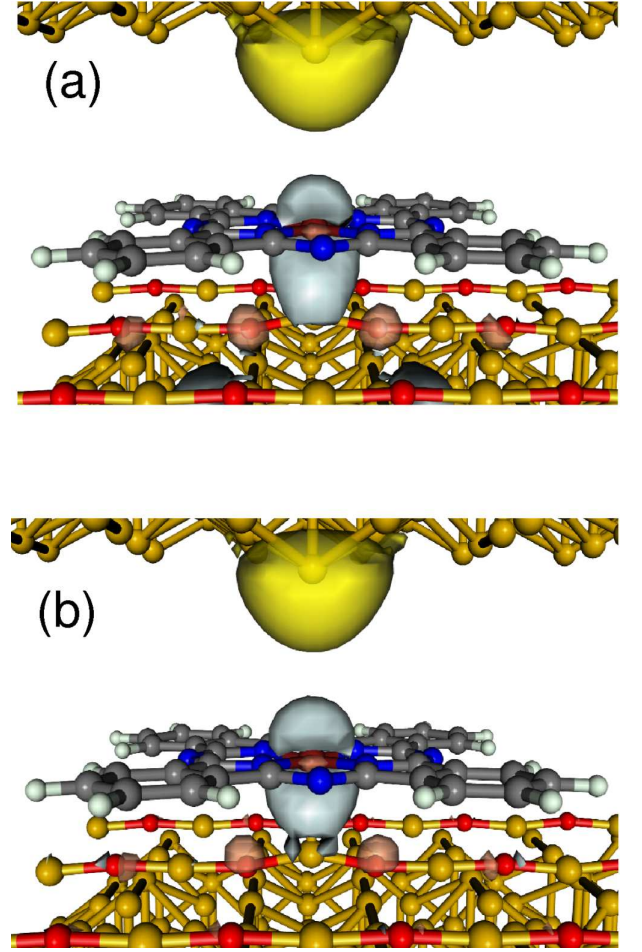


FIG. 5: Transmission eigenchannel corresponding to the largest transmission amplitude for (a) $E = E_F$ where E_F is the system's Fermi energy and (b) $E = E_F + 0.2$ eV. Light grey (light pink) color corresponds to the positive (negative) imaginary part of the eigenchannel amplitude coming from the STM tip. In gold color, the positive real part. Note that the isosurfaces were chosen different in (a) and (b) because of the large difference in transmission probability. The transmission channel exhibits a strong a_{1g} (d_{z^2}) character around the Fe atom.

due to the d_{z^2} Fe orbital, and that only the minority spin contributes to the tunneling transmission. In the transmission calculations, the tip-molecule distance was set at a small distance, 5 Å, with a large enough transmission probability to visualize the electron transmission eigenchannel easily.

This conclusion is further confirmed by computing the transmission eigenchannels. For that, we have used the INELASTICA code³⁹. The d_{z^2} orbital is the largest contributor to S-matrix eigenchannel dominating the transmission of electrons from the STM tip (here represented by an atom on a Cu(110) semi-infinite electrode) placed above the molecule. As can be seen in Fig. 5, the character of the dominant transmission eigenchannel is the same at the Fermi energy, E_F , Fig. 5(a) and at

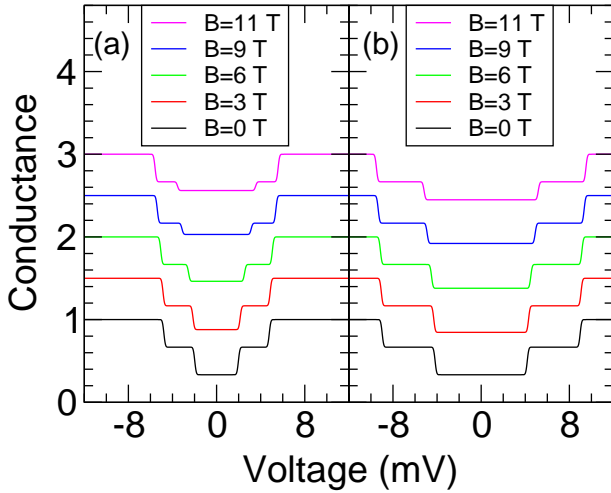


FIG. 6: Computed conductance for the (a) α and (b) β configuration of an adsorbed Fe-Pc molecule on a Cu(110)(2 \times 1)-O surface. The conductance has been normalized to 1 at large bias and the curves for the various B fields have been offset by 0.5 for representation purposes. The B field is oriented vertical to the sample with magnitude 0, 3, 6, 9 and 11 T as indicated in the graph.

$E = E_F + 0.2$ eV, Fig. 5 (b), the peak of the transmission resonance. These plots nicely correspond to the density plot of the Kohn-Sham eigenstate, Fig. 3.

C. Orbital picture of the electron tunnelling process

From the above DFT study, we can conclude that the Fe-Pc on a Cu(110)(2 \times 1)-O surface, is associated to the triplet electronic configuration $d_{xy}^2 d_{y'z}^2 d_{z^2}^1 d_{x'z}^1$ consistently with experiment⁴. The interaction between the d manifold and the surroundings is seen to split completely the d manifold, leading to five non-degenerate orbitals; the orbital angular momentum is then completely quenched, in the absence of significant spin-orbit couplings¹³ and this justifies the discussion, used in Ref.⁴ and here, of the magnetic anisotropy in terms of the spin angular momentum orientation. One can also notice that the Fe spin is also partially quenched from its free atom value ($S = 2$), again due to the interaction with the surroundings that induces a large upward energy shift of the $d_{x^2-y^2}$ orbital. The present DFT study also shows that when an STM tip is placed above the Fe atom, tunnelling dominantly involves the d_{z^2} (a_{1g}) orbital. So when an electron is sent from the tip on the Fe, it involves the $d_{xy}^2 d_{y'z}^2 d_{z^2}^1 d_{x'z}^1$ transient configuration, i.e. the total spin of the electron-adsorbate scattering intermediate is $S_T = 1/2$. Similarly, if a hole is sent from the tip to the Fe atom, tunnelling involves the $d_{xy}^2 d_{y'z}^2 d_{z^2}^0 d_{x'z}^1$ transient configuration, i.e. the total spin of the electron-adsorbate scattering intermediate is again $S_T = 1/2$. Thus, of the two possible symmetries for the electron-adsorbate scat-

tering ($S_T = 1/2$ or $3/2$), $S_T = 1/2$ is the prevailing symmetry in the tunnelling process.

In addition, transmission through the d_{z^2} orbital will dominate in a constant-current STM image and generate a bright spot at the Fe centre. This is consistent with the observation in Ref. [4] of the Fe-Pc molecule as a bright spot at the centre of a clover leaf. The bright spot corresponds to the d_{z^2} Fe orbital and the clover leaf is given by the contribution from other orbitals localized on the Pc ring (see in [34] a discussion of the link between bright M atoms in M-Pc STM images and their d orbitals). Furthermore, the magnetic transitions in this system were also found⁴ to be localized in the same region about the Fe atom, which we attribute to the d_{z^2} orbital.

D. Magnetic excitation processes

The inelastic conductance of the Fe-Pc has been computed using expression (10) for the α and β adsorption geometries, using the spin parameters determined in the DFT study. The conductance is shown in Fig. 6(a) for α configuration and Fig. 6 (b) for the β configuration, as a function of the STM bias for various values of the applied magnetic field, B , along the z -axis. The conductance has been normalized to 1 at large bias and the curves for the various B fields have been offset by 0.5. In the calculation, a Gaussian broadening of 0.25 meV was introduced to mimic various broadening effects. The conductance spectra resemble very much those measured by Tsukahara *et al.*⁴, with well-marked steps at the magnetic excitation thresholds (two inelastic thresholds for this $S = 1$ system because anisotropy splits the triplet state in three states⁴) and very significant contributions from the inelastic currents. Indeed, the conductance is dominated by inelastic tunnelling at large bias!

The differences between the α and β adsorption geometries are also well reproduced. One can also stress that, in the present approach, the magnetic excitations do not modify the maximum value of the global conductance C_0 , which is then independent of changes in the magnetic structure and in particular independent of the applied B field. This appears clearly in Figs. 6 (a) and (b) as well as in Fig. 2a and 2b of Ref. [4], confirming our view of the magnetic excitation process as a sharing of the global conductance over the various possible magnetic channels.

The relative magnitude of the elastic and inelastic channels in this system are further illustrated in Fig. 7 which presents the magnitude of the inelastic conductance steps for $C_0 = 1$. The two inelastic step heights are α_1 and α_2 (α_1 for the lowest threshold) for the α geometry (and similarly for the β one). The elastic conductance is then equal to the global conductance minus the inelastic ones, $(1 - \alpha_1 - \alpha_2)$ with this definition.

The present theoretical results as functions of the applied B field are compared with the data of Tsukahara *et al.*⁴. As a first remark, inelastic tunnelling contributes sig-

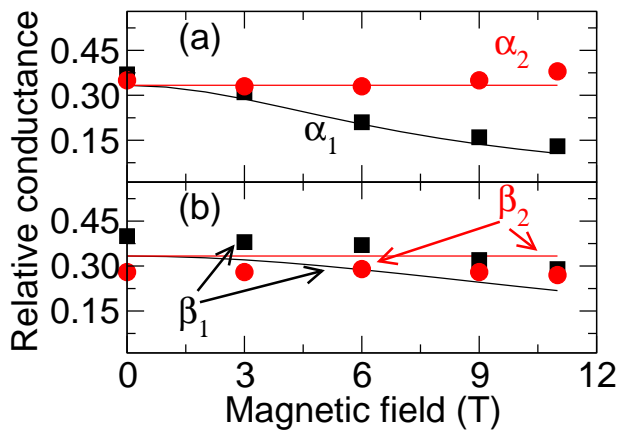


FIG. 7: Relative inelastic step heights in the conductance as a function of the magnetic field B , for (a) α and (b) β configurations. α_1 and α_2 refer to the first and second excitation steps for the α configuration respectively. Analogously, β_1 and β_2 refer to the first and second excitation steps for the β configuration. The experimental data points are represented with black squares for the first excitation and as red circles for the second one and are taken from the supplemental material of Ref. [4].

nificantly to the tunnelling current: typically for $B = 0$ T, the inelastic current is equal to twice the elastic current. Second, we can see that the present theoretical results reproduce very well the relative magnitude of the three contributions to the conductance (elastic and two inelastic). In particular, the variation with B is well accounted for.

The variation of the strength of the magnetic excitation with B is in fact reflecting the change of the magnetic structure of the adsorbate. For $B = 0$, the structure of the conductance curve is due to the anisotropy imposed by the substrate to the Fe-Pc molecule; although the level positions are different in the α and β adsorption geometries, the eigenstates of Hamiltonian (1) at $B = 0$ are the same in both geometries (see Tsukahara *et al.*⁴) and consequently, the excitation probabilities are the same, as seen in Fig. 7. The effect of a finite B field is to decouple the Fe-Pc spin from the substrate and to tend to a Zeeman limit at large B . This decoupling is easier for the α -geometry, because of a weaker transversal anisotropy E (given above). In the limit of very large B (not fully reached here), the ϕ_n states reduce to $|S, M\rangle$ states with the ground state corresponding to $M = -1$. The only allowed transition is to the ($M = 0$) excited state, so that only one inelastic step remains in the conductance spectrum. Its height is given by the modulus square of a Clebsch-Gordan coefficient and in this limit, the inelastic current is equal to one third of the total current.

IV. MAGNETIC TRANSITIONS IN SUPPORTED Co-PHTHALOCYANINE MOLECULES

Superposed layers of Co-Pc molecules on Pb(111) islands were studied experimentally by magnetic IETS and revealed the existence of superexchange interactions⁵. Magnetic excitation of the Co-Pc molecules were observed but only for several adsorbed layers of Co-Pc molecules. No excitation was observed in the single layer case, suggesting that either the spin of the Co-Pc molecular layer lying directly on the Pb surface was quenched by the interaction with the substrate or the possible magnetic excitations were very short lived⁵. The Co-Pc spin was found to be $S = 1/2$, and when several layers are stacked one on top of each other, with a stacking angle of 60° , the spins of the Co-Pc molecule in the second and outer layers couple together in a way well-described by a Heisenberg Hamiltonian, with an anti-ferromagnetic exchange coupling, J , of the order of 18 meV ⁵.

Very strong magnetic excitations were reported in the multi-layer case⁵. The present formalism can be used to predict the magnitude of the magnetic excitation in such systems. If we neglect the magnetic anisotropy of adsorbed Co-Pc, the only ingredients in our approach are the adsorbate spin S , the intermediate total spin S_T , and the anti-ferromagnetic interaction J for the stacked molecules. Both S and J are known from experiment⁵. We did not perform a detailed DFT study as for the Fe-Pc case. We assumed that we can extrapolate the electronic structure from Fe-Pc to Co-Pc³⁵, in both cases the Pc molecules being partly decoupled from the underlying metal. As discussed in Ref. 35, an M-Pc series is formed by the various incomplete d -shell metals and the Co structure corresponds to adding a d electron to the Fe case. With the open shell structure of Fe-Pc outlined above ($d_{xy}^2 d_{y'z}^2 d_{z'z}^1 d_{x'z}^1$), this leads to a doublet configuration of the Co-Pc electronic structure, independently of the orbital in which the electron is added. This is perfectly consistent with the experimental observation. Then, we can assume that tunnelling involves minority spin electrons because the molecular electronic structure at the Fermi level is given by the last partially-occupied d orbital also in this case. Hence, the intermediate spin state is $S_T = 0$, both for electrons and holes.

In the case of a single active Co-Pc molecule (two adsorbed layers), an applied magnetic field is needed to perform a magnetic IETS experiment, because of the molecular spin $S = 1/2$, see Ref. [5]. For a finite B field, a Zeeman splitting corresponding to a Landé factor 1.88 has been observed⁵. Assuming a simple Zeeman structure, i.e. no magnetic anisotropy induced by the substrate, the above formalism, at finite B , predicts a single inelastic peak with an inelastic current equal to the elastic current (note that this result is independent of the value of the Landé factor). This is consistent with the observations⁵, which reported an increase of the current around 110-120 % at the inelastic threshold (see Fig. 2c in Ref. [5]).

In the case of three molecular layers, two stacked molecules in the upper two layers interact via an anti-ferromagnetic coupling, so that the ground state of the two-molecule system is a spin 0 state while the spin 1 states are excited states (we neglect a possible anisotropy induced by the substrate). Magnetic excitations of the system by tunnelling electrons for a vanishing B have been observed experimentally as a sharp step in the conductance⁵. The above formalism predicts at $B = 0$, in the absence of any anisotropy induced by the substrate, a single conductance step at finite bias (the transition from $S = 0$ to $S = 1$), the inelastic current being three times larger than the elastic one. An accurate quantitative comparison with experiment of the step height is difficult because of the non-flat behaviour of the global conductance in this system (see Ref. [5]); nevertheless, our prediction of a 300 % increase of the conductance at the inelastic threshold is in good agreement with the experimental data. For finite B , the $S = 1$ excited states split into a Zeeman structure and the present formalism predicts three steps in the conductance, each of them with a height equal to the elastic conductance. Again, this Zeeman limit corresponds to what is observed experimentally for large B (see e.g. Fig. 3b in Ref. [5]). As the main feature of this system, one can stress the extremely large contribution of the inelastic current compared to that of the elastic current in the total current: the present theory predicts a total inelastic current three times larger than the elastic one, in good agreement with what is observed experimentally. One can also emphasize that in the Co-Pc case, we only discuss the Zeeman structure limit, so that the only ingredients in our approach are the value of the local spin ($S = 1/2$) and of the spin of the electron+adsorbate system ($S_T = 0$) and all the predictions of relative magnitudes of elastic and inelastic currents are directly obtained from Clebsch-Gordan coefficients.

V. SUMMARY AND CONCLUDING REMARKS

The orientation of the magnetic moment of individual adsorbates on a surface leads to a magnetic structure with excitation energies in the few meV range. Recent experimental developments in the low-Temperature Inelastic Electron Tunnelling Spectroscopy allowed the direct observation of transitions among these magnetic states in the case of magnetic atoms adsorbed on a metal with a decoupling coating in between. The present paper reports a theoretical study of magnetic excitations induced by tunnelling electrons in metal-phthalocyanine molecules adsorbed on surfaces (Fe-Pc on Cu(110)(2×1)-O and Co-Pc stacked on Co-Pc on Pb) that have been the subject of recent experimental studies^{4,5}. It is based on a theoretical framework recently introduced¹⁷ to treat tunnelling electron-induced magnetic transitions and on a DFT calculation to characterize the electronic structure of the Fe-Pc molecule on Cu(110)(2×1)-O system.

Our approach determines the strength of the magnetic transitions induced by tunnelling electrons when the STM tip is placed on top of the magnetic atom. The input ingredients in our calculations are the magnetic Hamiltonian describing the interaction of the adsorbate magnetic moment with its environment and the total spin of the tunnelling electron-adsorbate system. The magnetic Hamiltonian has been taken from its parameterisation using the experimental results on the energy spectrum of magnetic levels^{4,5}. In the Fe-Pc on Cu(110)(2×1)-O case, a DFT study determined the electronic structure of the adsorbed Fe-Pc molecule together with the symmetry and spin structure of the tunnelling electron. An excellent account of the experimental findings was obtained; in particular, the extremely large magnetic excitation probabilities (inelastic contribution dominating over the elastic one in the tunnelling current) were confirmed.

The Fe atom in the adsorbed Fe-Pc has electronic and magnetic structures quite different from those of a free Fe atom and of Fe adsorbed on CuN studied earlier^{3,17}. The interaction of the d -manifold with the Pc ring and with the CuO substrate results in a full splitting of the manifold and in a spin state different from the atomic case. Then a Fe atom inside an adsorbed Fe-Pc molecule⁴ appears very differently in a magnetic IETS experiment compared to the case of an adsorbed Fe atom³.

The magnetic transitions appear to be much more probable than other inelastic processes studied earlier, such as vibrational excitation of the adsorbate¹⁰⁻¹². In the most spectacular case (Co-Pc, see above and Ref. [5]), the inelastic contribution to the tunnelling current is three times larger than the elastic one. The present approach explains this striking difference. Since electron tunnelling occurs on a short time scale compared to magnetic anisotropy, one can treat electron tunnelling independently of the magnetic anisotropy in the sudden approximation. The magnetic transitions then appear as the result of a change of coupling scheme for the adsorbate spin: coupling to the adsorbate environment in the initial and final states and coupling to the tunnelling electron spin via exchange interactions for the tunnelling process. The strength of the magnetic transitions is then determined by spin coupling coefficients (such as e.g. Clebsch Gordan coefficients) and the present approach reduces to computing how a magnetism-independent tunnelling current is shared among the various magnetic states, i.e. how a total magnetism-independent current is shared between elastic and inelastic parts. The importance of a given magnetic transition is then linked to the weight of the initial and final states in the magnetism-independent collision intermediate and it can thus be very large. In particular, it does not depend on the strength of an interaction coupling initial and final states during electron tunnelling. Our approach is, thus, perfectly well-adapted to treat situations like the present ones, where tunnelling appears to be dominated by inelastic effects.

The strength of the magnetic transitions thus appears to be the direct consequence of the spin coupling scheme of the system. The variation of the magnetic transitions with an applied magnetic field, B , follows the variation of the adsorbate magnetic structure with B , basically the switch from a magnetic anisotropy induced by the adsorbate environment to a Zeeman structure, i.e. the decoupling of the adsorbate spin from its environment by the B -field action (see e.g. Fig. 6). In this way, the present study of the magnetic transitions strength as a function of B further strengthens the knowledge of the adsorbate magnetic structure as it can be derived from the analysis of the experimental energy spectrum of the magnetic states. Basically, the analyses of the strength of the magnetic transitions and of the energy spectrum are probing the same properties of the system.

Acknowledgments

We are grateful to Prof. Noriaki Takagi and Prof. Maki Kawai for extended discussions on the experimental data. We thank Prof. Magnus Paulsson for his help in some of the calculations. Financial support from the spanish MICINN through grant FIS2009-12721-C04-01 is gratefully acknowledged. N.L. thanks Université Paris-Sud for an Invited Professorship and for its hospitality. F.D.N. would like to thank the Centro de Supercomputación de Galicia (CESGA) for providing computational resources.

- ¹ A. J. Heinrich, J. A. Gupta, C. P. Lutz and D. M. Eigler, *Science* **306**, 466 (2004).
- ² C. F. Hirjibehedin, C. P. Lutz and A. J. Heinrich, *Science* **312**, 1021 (2006).
- ³ C. F. Hirjibehedin, C.-Y. Lin, A. F. Otte, M. Ternes, C. P. Lutz, B. A. Jones and A. J. Heinrich, *Science* **317**, 1199 (2007).
- ⁴ N. Tsukahara, K. Noto, M. Ohara, S. Shiraki, N. Takagi, Y. Takata, J. Miyawaki, M. Taguchi, A. Chainani, S. Shin and M. Kawai *Phys. Rev. Lett.* **102**, 167203 (2009).
- ⁵ Xi Chen, Y.-S. Fu, S.-H. Ji, T. Zhang, P. Cheng, X.-C. Ma, X.-L. Zou, W.-H. Duan, J.-F. Jia and Q.-K. Xue, *Phys. Rev. Lett.* **101**, 197208 (2008).
- ⁶ C. Iacovita, M. V. Rastei, B. W. Heinrich, T. Brumme, J. Kortus, L. Limot and J. P. Bucher, *Phys. Rev. Lett.* **101**, 116602 (2008).
- ⁷ Y.-S. Fu, T. Zhang, S.-H. Ji, X. Chen, X.-C. Ma, J.-F. Jia and Q.-K. Xue, *Phys. Rev. Lett.* **103**, 257202 (2009).
- ⁸ T. Balashov, T. Schuh, A. F. Takacs, A. Ernst, S. Ostanin, J. Henk, I. Mertig, P. Bruno, T. Miyamachi, S. Suga and W. Wulfhchel, *Phys. Rev. Lett.* **102**, 257203 (2009).
- ⁹ F. D. Novaes, N. Lorente and J.-P. Gauyacq, *to be published*.
- ¹⁰ B. C. Stipe, M. A. Rezai, and W. Ho, *Science* **280**, 1732 (1998).
- ¹¹ W. Ho, *J. Chem. Phys.* **117**, 11033 (2002).
- ¹² T. Komeda, *Progress in Surf. Sci.* **78**, 41 (2005).
- ¹³ K. Yosida *Theory of magnetism*, Springer series in solid-state science (Springer, Berlin, Heidelberg, 1996)
- ¹⁴ J. Fransson, *Nano Lett.* **9**, 2414 (2009).
- ¹⁵ J. Fernández-Rossier, *Phys. Rev. Lett.* **102**, 256802 (2009).
- ¹⁶ M. Persson, *Phys. Rev. Lett.* **103**, 050801 (2009).
- ¹⁷ N. Lorente and J.-P. Gauyacq, *Phys. Rev. Lett.* **103**, 176601 (2009).
- ¹⁸ R.A.Abram and A.Herzenberg, *Chem. Phys. Lett.* **3**, 187 (1969).
- ¹⁹ D. Teillet-Billy, J.-P. Gauyacq and M. Persson, *Phys. Rev. B* **62**, R 13306 (2000).
- ²⁰ D. Teillet-Billy, L. Malegat and J.-P. Gauyacq, *J. Phys. B* **20**, 3201 (1987).
- ²¹ B. Bahrim, D. Teillet-Billy and J.-P. Gauyacq, *Phys. Rev. B* **50**, 7860 (1994).
- ²² J.W. Gadzuk, *J. Chem. Phys.* **79**, 3982 (1983).
- ²³ V. Djamo, D. Teillet-Billy and J.P. Gauyacq, *Phys. Rev. Lett.* **71**, 3264, (1993).
- ²⁴ N. Lorente and M. Persson, *Phys. Rev. Lett.* **85**, 2997 (2000).
- ²⁵ N. Lorente, *App. Phys. A* **78**, 799 (2004).
- ²⁶ M. Paulsson, T. Frederiksen, H. Ueba, N. Lorente and M. Brandbyge, *Phys. Rev. Lett.* , 226604 (2008).
- ²⁷ G. J. Schulz, *Rev. Mod. Phys.* **45**, 423 (1973).
- ²⁸ D.J. Birtwistle and A. Herzenberg, *J. Phys. B* **4**, 53 (1971).
- ²⁹ A. J. Mayne, F. Rose and G. Dujardin, *Faraday Discuss.* **117**, 241 (2000).
- ³⁰ M. Cizek, M. Thoss, and W. Domcke, *Phys. Rev. B* **70**, 125406 (2004).
- ³¹ S. Monturet and N. Lorente, *Phys. Rev. B* **78**, 035445 (2008).
- ³² B. C. Stipe, M. A. Razaei and W. Ho, *Science* **279**, 1907 (1998).
- ³³ B. W. Dale, R. J. P. Williams, C. E. Johnson and T. L. Thorp, *J. Chem. Phys.* **49**, 3441 (1968).
- ³⁴ X. Lu and K. W. Hipps, *J. Phys. Chem. B* **101**, 5391 (1997).
- ³⁵ M. S. Liao and S. Scheiner, *J. Chem. Phys.* **114**, 9780 (2001).
- ³⁶ J. M. Soler, E. Artacho, J. D. Gale, A. Garcia, J. Junquera, P. Ordejon, D. Sanchez-Portal, *J. Phys.: Condens. Matter* **14**, 2745 (2002).
- ³⁷ M. Brandbyge, J. L. Mozos, P. Ordejon, J. Taylor and K. Stokbro, *Phys. Rev. B* **65**, 165401 (2002); F. D. Novaes, A. J. R. da Silva and A. Fazzio, *Brazilian Journal of Physics*, **36**, 799 (2006). Starting from version 3.0b, SIESTA includes the TRANSIESTA module, see <http://www.icmab.es/siesta/>
- ³⁸ J. Perdew, K. Burke, and M. Ernzerhof, *Phys. Rev. Lett.* **77**, 3865 (1996).
- ³⁹ T. Frederiksen, M. Paulsson, M. Brandbyge and A.-P. Jauho, *Phys. Rev. B* **75**, 205413 (2007); M. Paulsson and M. Brandbyge, *Phys. Rev. B* **76**, 115117 (2007). The source code can be downloaded from <http://sourceforge.net/projects/inelastica>